BOLETIN DE LA SOCIEDAD ESPAÑOLA DE
Cerámica y Vidrio
A R T I C U L O

Ferrites nanoparticles MFe_2O_4 (M = Ni and Zn): hydrothermal synthesis and magnetic properties

R. SAEZ PUCHE[1], M. J. TORRALVO FERNANDEZ[1], V. BLANCO GUTIERREZ[1], R. GOMEZ[2], V. MARQUINA[2], M.L. MARQUINA[2], J.L. PEREZ MAZARIEGO[2] , R. RIDAURA[2].

[1]Departamento de Química Inorgánica, Facultad de Química, Universidad Complutense, Madrid, España.
[2]Departamento de Física, Facultad de Ciencias, Universidad Nacional Autónoma de México, México D.F., México

MFe_2O_4 (M = Ni and Zn) nanoparticles were prepared by the hydrothermal method. The obtained samples were characterized by X-ray and electron diffraction, Scanning and Transmission Electron Microscopy and Mössbauer spectroscopy. The transmission images show homogeneous shape and particle size ranging from 10 to 40 nm, depending on the nature of the M cation. Mössbauer spectroscopy yields to a ratio of occupancy between the A and B sites of 0.7 in the case of $NiFe_2O_4$ oxide. DC magnetization (2-300 K) measurements reveal a superparamagnetic behaviour for the $ZnFe_2O_4$ sample with a blocking temperature of 20 K. By contrast, in the case of the $NiFe_2O_4$ ferrite the blocking temperature appears to be above 300 K and at lower temperature, it shows a ferrimagnetic behaviour arising from the superexchange interactions that take place in this inverse spinel. Mössbauer spectroscopy results confirm the bulk magnetic measurements.

Keywords: ferrites, nanoparticles, superparamagnetism, ferrimagnetism, inverse spinel.

Nanopartículas de ferrita MFe_2O_4 (M = Ni y Zn): síntesis hidrotermal y propiedades magnéticas.

Se han preparado mediante el método hidrotermal nanopartículas de ferritas MFe_2O_4 (M = Ni, Zn). Las muestras obtenidas fueron caracterizadas mediante difracción de rayos X y electrones, microscopía electrónica de transmisión y barrido y espectroscopia Mössbauer. Las imágenes de transmisión muestran partículas de forma y tamaño homogéneo de 10 a 40 nm según la naturaleza del catión M. La espectroscopia Mössbauer revela una relación de ocupación entre los sitios A y B por los átomos de hierro de 0.7 en el caso del óxido $NiFe_2O_4$.
Las medidas de magnetización DC (2 – 300 K) muestran un comportamiento superparamagnético para la muestra $ZnFe_2O_4$ con una temperatura de bloqueo de 20 K. En el caso de las nanopartículas de $NiFe_2O_4$ la temperatura de bloqueo parece estar por encima de los 300 K mostrando por debajo de la misma, comportamiento ferrimagnético provocado por las interacciones de superintercambio que tienen lugar en esta espinela inversa. Los resultados de espectroscopia Mössbauer confirman los datos de las medidas magnéticas.

Palabras clave: ferritas, nanopartículas, superparamgnetismo, ferrimagnetismo, espinela inversa.

1. INTRODUCTION

Synthesis of nanosized magnetic particles is namely gaining interest in material processing technologies and the fabrication of novel materials (1-3). These nanosized magnetic particles exhibit very interesting properties that made of them promising candidates to be used in different applications such as high density recording, ferrofluids, high frecuency devices, magnetic refrigerators and new pigments (4,5). Concerning the properties of these magnetic particles, namely coercivity, magnetic saturation, remanence and loss, change dramatically as the size of the particles move down into the nanometric range (6, 7). Moreover, there are numerous reports wherein anomalies have been reported in the structural and magnetic properties of different spinel ferrites in the nanoscale (8, 9). In this sense, the zinc ferrite is a normal spinel exhibiting antiferromagnetism with a Neel temperature of 10.5 K. The ordering temperature can be raised by increasing Fe^{3+} population at A sites through mechanical activation (10, 11) giving rise to the so called mixed spinel with partial inversion. For inverse spinel the antiferromagnetic A-B superexchange interactions are stronger compared to intersublattice A-A and B-B ones, giving rise to considerably higher ordering temperatures (12,13).

However, nanoparticles of zinc ferrite prepared using different methods of synthesis have different ferrimagnetic characteristics showing a great variety of Neel temperature, coercive fields and saturation moments depending on the particle size (14, 15). Hence, the synthesis of zinc ferrite as nanoparticles and the study of their magnetic properties as a function of the shape and size is an active and interesting area of research in the field of the material science.

In the present paper, zinc and nickel ferrites were prepared by using the hydrothermal method at low temperature which yields nanoparticles with uniform size. These nanoparticles have been fully characterized and the study of their magnetic properties is one of the aims of this work.

2. EXPERIMENTAL

MFe_2O_4 (M = Ni and Zn) nanoparticles were prepared by the hydrothermal method in which stoichiometric amounts of iron and zinc or nickel nitrates were disolved in distilled water obtaining a yellow solution. By adding a KOH 2 M solution until pH = 11 the iron and zinc or nickel hydroxides were precipitated. This precipitate was transferred into a Teflon stainless-steal autoclave and heated for different periods of time, ranging from 3 hours to 15 hours at 160 ºC to obtain Zn-ferrite and 180 ºC in the case of Ni-ferrite. The final product was filtered and washed with distilled water and ground after drying in air.

Bulk $ZnFe_2O_4$ sample was also prepared by using the conventional ceramic method, where the stoichiometric amounts of zinc and iron nitrates were heated in air at 900ºC for 12 hours.

X–ray powder diffraction patterns were recordered in a Siemens kristalloflex 810 diffractometer and D–5000 goniometer equipped with a graphite monochromator and Cu kα radiation.

The transmission electron microscopy (TEM) study was performed in a JEOL 2000 electron microscope working at 200 kV. Scanning electron micrographs (SEM) were taken in a JEOL 6400 electron microscope working at 20 kV.

Magnetic susceptibility and magnetization measurements were done in a Quantum Design XL-SQUID magnetometer in the temperature range of 2-300 K at different magnetic fields up to 5 T. Magnetic susceptibility measurements were performed after the sample was cooled at 2K in zero field cooling (ZFC). In the so called field cooling measurements modality (FC) the sample was cooled in presence of the requiered magnetic field down to 2K.

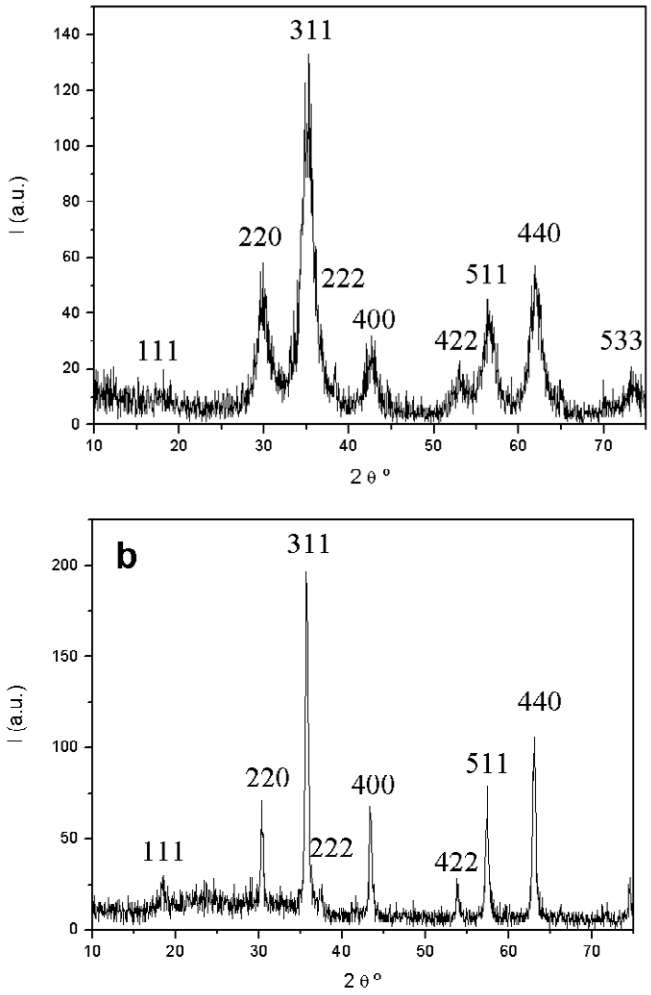

Fig. 1. X-ray diffraction patterns of $ZnFe_2O_4$ (a) and $NiFe_2O_4$ (b).

3. RESULTS AND DISCUSSION

3.1 Structural and microstructural characterization.

X–ray diffraction data (Figure 1) reveal that all the samples crystallize with the cubic spinel type structure, space group Fd3m, and permit us to exclude the presence of any impurities or secondary phases. The lattice parameter determined via least –square method are a = 8.449 (6) Å and a = 8.339 (5) Å for the $ZnFe_2O_4$ and $NiFe_2O_4$ respectively. The broadening of the reflections indicates the nanometric size of the particles for both samples. The average particle size has been calculated using the well-known Scherrer's formula (16), $t = (0.9\,\lambda)/(\beta \cos\theta)$, where t is the crystalline size, λ the wavelength (Cu Kα), θ the Bragg angle and β the full width to half maximum of the (311) reflection on the MFe_2O_4 cell. A range size from 6 nm to 10 nm was obtained for $ZnFe_2O_4$ and from 50 nm to 60 nm for the nickel ferrite.

Figure 2 shows TEM images and electron diffraction patterns of Zn-ferrite (a) and Ni-ferrite (b).Typical octahedral-shaped particles are visualized by TEM for both samples but just the Zn-ferrite shows a more homogenous particle size (figure 2a). The average size estimated from the image of about 60 particles of each sample was 10 nm in the case of the Zn-ferrite and 40 nm for the Ni-ferrite, in good agreement with the values obtained from the X-ray powder data. In the insets are shown selected area electron diffraction (SAED) patterns corresponding to the $ZnFe_2O_4$ nanoparticles (figure 2a) and a $NiFe_2O_4$ octahedra projected along the [111] direction (figure 2b). The electron diffraction results, as the X-ray patterns, indicate single phase for both Zn-ferrite and Ni-ferrite and the high intensity of the diffraction maxima reveal that well crystalline samples have been obtained in both cases. It is worth noting that the samples produced by the ceramic method (figure 3) are formed by bigger particles

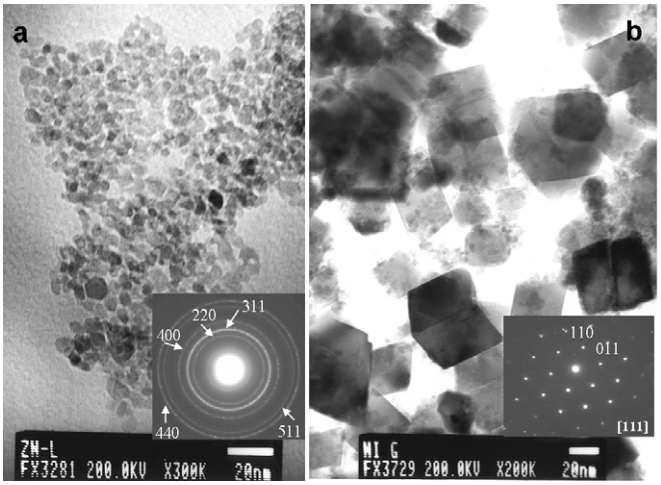

Fig. 2. TEM images and SAED patterns (shown in the insets) of $ZnFe_2O_4$ and $NiFe_2O_4$ (b).

than those prepared by hydrothermal synthesis and in the first case the samples also present less homogenous particle size distributions.

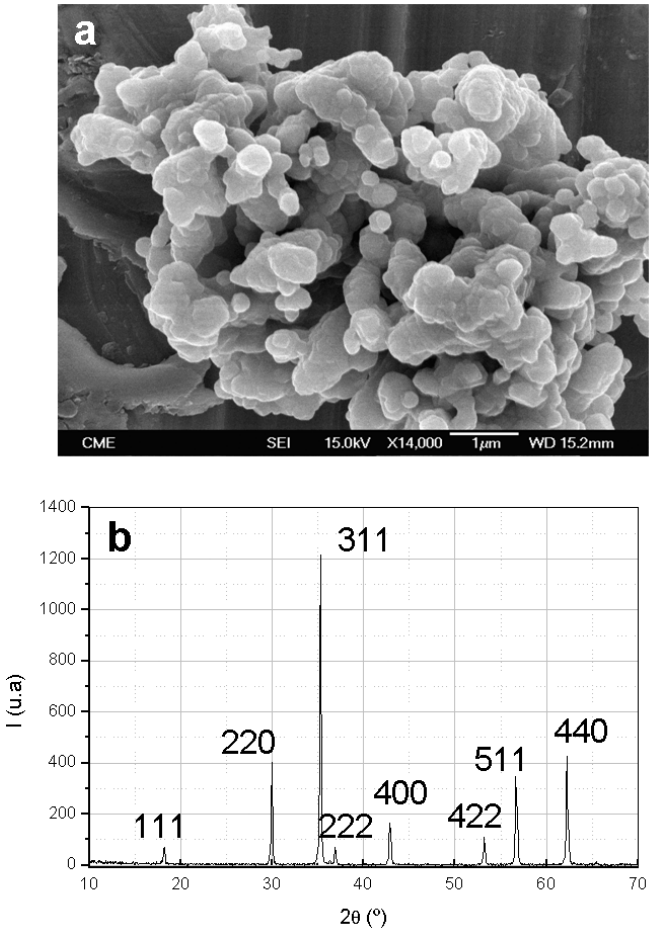

Fig. 3. SEM image (a) and x-ray diffraction pattern (b) of $ZnFe_2O_4$ prepared by the ceramic method.

3.2 Magnetic properties.

Figure 4a shows the temperature dependence of magnetic susceptibility in the ZFC-FC processes with an applied field H = 500 Oe for the $ZnFe_2O_4$ spinel. It can be observed a deviation of the FC from ZFC susceptibility measurements below 10 K. While the latest exhibits a broad maximum centered at 20 K, χ_{FC} remains almost constant down to 2 K. This type of feature is typically observed in superparamagnetic fine particles. This temperature corresponding to the maximum is called blocking temperature (T_B) and above 20 K superparamagnetic behaviour is observed. It has been recently reported a progresive increase of T_B with the inversion degree and the size of the particles (17). Both χ_{FC} and χ_{ZFC} are coincident above the T_B.

Figure 4b shows the variation of the reciprocal susceptibility as a function of the temperature for the $ZnFe_2O_4$ sample. It can be observed that the susceptibility obeys a Curie-Weiss behaviour over a very narrow temperature range, 200-300K, showing a positive value of the Weiss temperature as high as 130K. This result combined with the values of the magnetization obtained at low temperatures (figure 4a) is consistent with the presence of a ferrimagnetic behaviour arising from the partially inverse character of this $ZnFe_2O_4$ spinel.

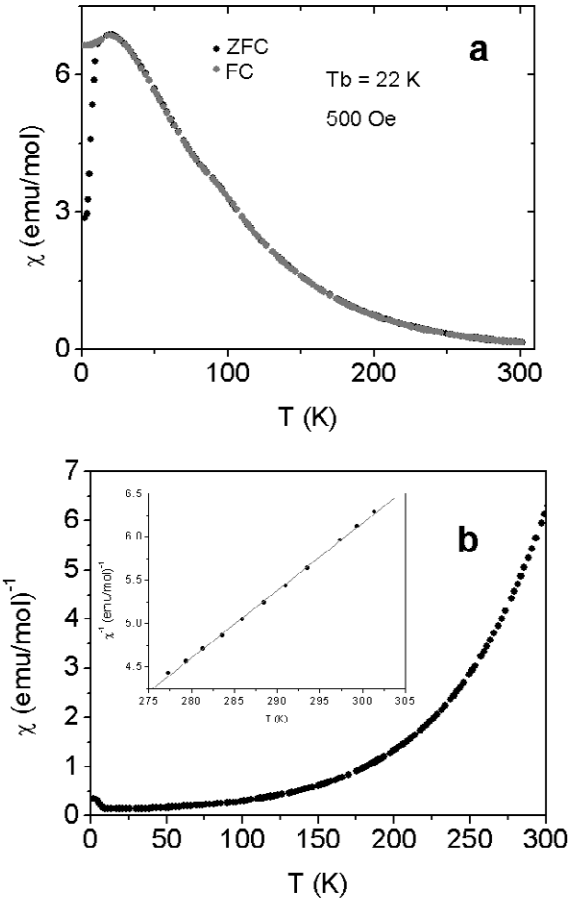

Fig. 4. ZFC-FC curves (a) and susceptibility as a function of temperature (b) corresponding to $ZnFe_2O_4$ sample.

Magnetization as a function of the magnetic field up to 50 KOe at different temperatures is shown in figure 5a. It can be observed the typical behaviour of a magnetic state with spontaneous magnetization in which the magnetic moment decreases when the temperature is increased, and takes a value of zero at 250 K, where these ferrites behave as superparamagnetic. This behaviour is confirmed from the magnetization curve obtained a 250 K (figure 5) where the coercive field and remanence are zero. This indicates that these $ZnFe_2O_4$ nanoparticles behave as superparamagnetic at 250 K. However, below the blocking temperature, the particles do not have enough energy to reach the thermal equilibrium and the hysteresis appears.

Figure 6a shows the thermal variation of the magnetic susceptibility for the $NiFe_2O_4$ sample. It can be observed a marked irreversibility in the FC and ZFC curves although the blocking temperature (T_B) at which the irreversibility occurs is almost outside of the range of measurements. Hysteresis loops figure 6b, reveal a ferrimagnetic behaviour below T_B = 250 K with a saturated magnetic moment of about 2.2 μ_B which well agrees the total inversion of the ground state in this spinel. However, above the T_B the coercive field is almost zero which justifies the superparamagnetic behaviour of this nanosized $NiFe_2O_4$ ferrite.

On the other hand our preliminary room temperature Mössbauer spectra for these two Ni and Zn ferrites (figure 7) confirm the results obtained from the bulk magnetic

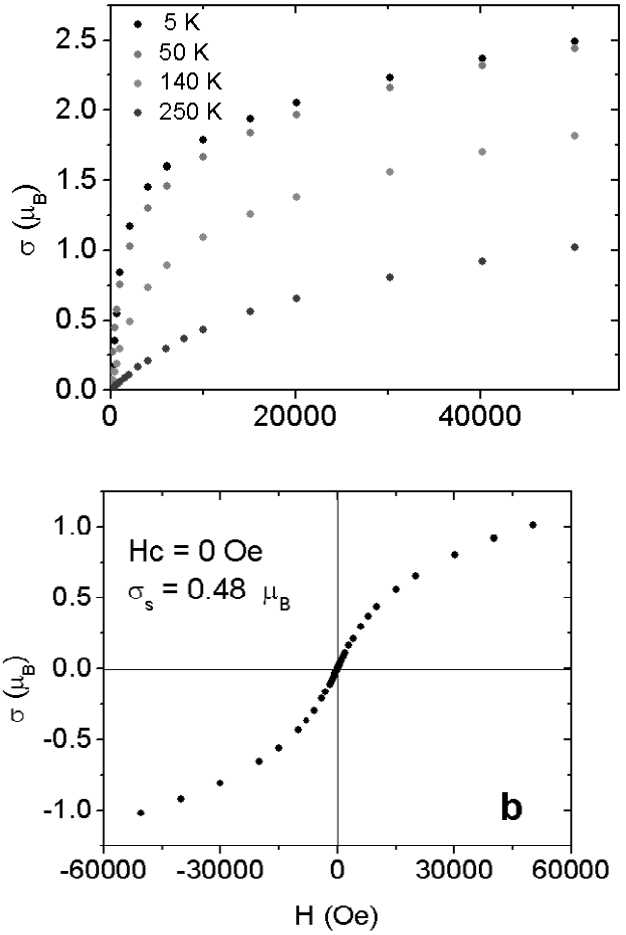

Fig. 5. Magnetization as a function of the magnetic field at different temperatures (a) and magnetization loop obtained at 250K (b) for $ZnFe_2O_4$ sample.

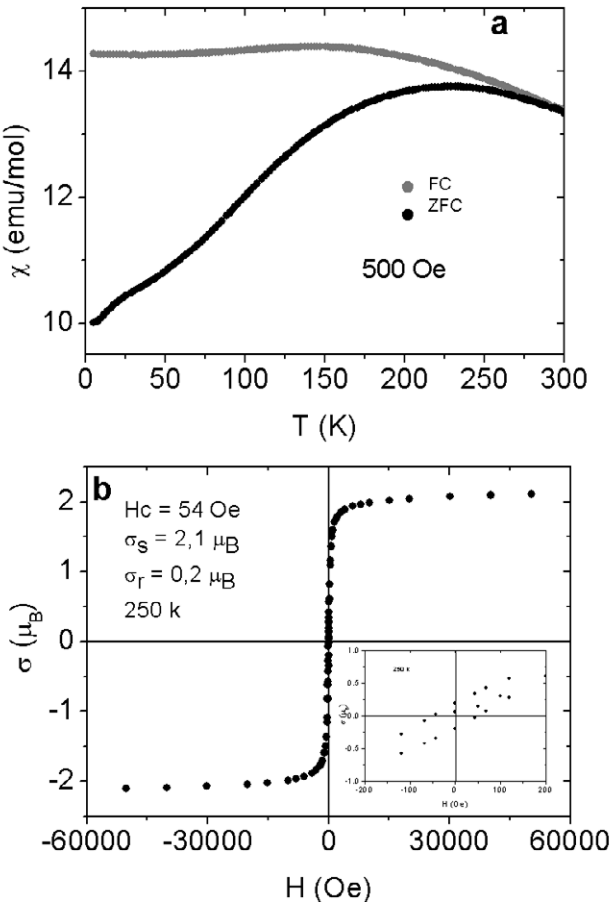

Fig. 6. ZFC-FC curves (a) and magnetization loop obtained at 250K (b) for $NiFe_2O_4$ sample.

measurements discussed above. In the case of the $ZnFe_2O_4$, (figure 7a) the spectra has been fitted by considering one Lorentzian doublet which confirms the superparamagnetism character of this spinel. However, the lack of resolution in the spectrum does not allow us to evaluate quantitatively the Fe population in the A and B sites of the spinel. The Mössbauer spectrum for $NiFe_2O_4$ is given in figure 7b where it can be observed that the data have been fitted by considering two Lorentzians sextets. The shape of these sextets reveal the existence of at least two magnetic components, see Table I. The subspectrum which presents the highest hyperfine magnetic field of 505.6 KOe corresponds to the Fe in B-sites while the subspectrum b can be assigned to the Fe in A-sites. The determined Fe site population for the tetrahedral (A) and octahedral (B) is 41% and 59% respectively.

4. CONCLUSIONS

MFe_2O_4 (M = Ni, Zn) oxides have been prepared as single phase by the hydrothermal method. For similar synthesis conditions, the particle size depends on the nature of the M element. The Zn-ferrite presents smaller particles (average size of 10 nm) and more homogenous size. For Ni-ferrite most of particles are well-formed octahedra with mean size of 40 nm. $ZnFe_2O_4$ behaves as superparamagnetic showing blocking temperature of 20 K while $NiFe_2O_4$ presents blocking

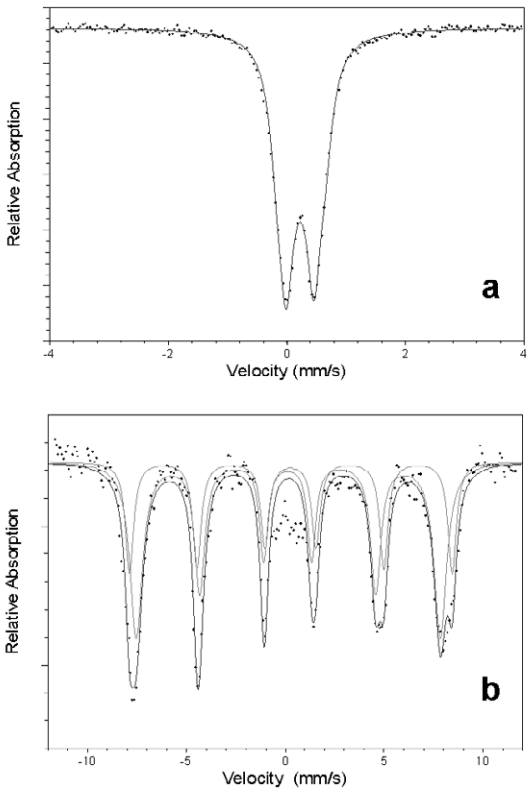

Fig. 7. Room temperature Mössbauer spectra for $ZnFe_2O_4$ (a) and $NiFe_2O_4$ (b) nanoparticles.

Table1. Results of $^{57}Fe^{3+}$ Mössbauer measurements at room temperature on $ZnFe_2O_4$ and $NiFe_2O_4$ samples.

$ZnFe_2O_4$	IS (mm/s)	ΔQ (mm/s)	H (kOe)	Γ (mm/s)
Doublet1	0.2315(2)	0.01	25.15(51)	0.15

$NiFe_2O_4$	IS (mm/s)	ΔQ (mm/s)	H (kOe)	Γ (mm/s)
Sextet 1	0.147(12)	0.000(12)	474.9(10)	0.25
Sextet 2	0.241(16)	0.01	505.6(14)	0.25

Site Populations (%)
Sextet 1 59.3(27)
Sextet 2 40.7205

temperature above room temperature. Below the blocking temperature, these ferrites present ferrimagnetic behaviour arising from the total inversion of the ground state in $NiFe_2O_4$ and the partially inverse character in the case of $ZnFe_2O_4$.

ACKNOWLEDGMENTS

This work has been financed by MEC, project MAT2006-13459-C01-02.

REFERENCES

1. G. Skaudan, Y. J. Chen, N. Glumar, B. H. Kear, Synthesis of oxide nanoparticles in low pressure flames, Nanostructured materials. 11, 149-153 (1999)
2. S. Gangopadhyay, Hadjipanayis, B. Dale, C.M. Sorenson, K.J. Klabunde, V.Papaefthymiou, A. Kostikas, Magnetic properties of ultrafine iron particles, Phys. Rev. B, 45, 9778-9787 (1992)
3. L.P. Li, G.S. Li, R.L. Smith, H. Honomata, Microstructural evolution and magnetic properties of $NiFe_2O_4$, Chem. Mater., 12, 3705-3714 (2000)
4. D.H.Han, H.L. Luo, Z. Yang, Remanent and anisotropic switching field distribution of platelike Ba-ferrite and acicular particulate recording media, J. Magn. Magn. Mater., 161, 376-378 (1996)
5. R.A. Candeia, M.A.F. Souza, M.I.B. Bernardi, S.C. Maestrelli, I.M.G. Santos, A.G.Souza, E. Longo, $MgFe_2O_4$ pigment obtained at low temperature, Mater. Res. Bull., 41, 183 (2006)
6. I.M.L.Billas, A. Chatelain, W.A. der Heer, Magnetism from the atom to the bulk in Iron, Cobalt and Nickel clusters, Science, 265, 1682-1684 (1994)
7. D.D. Awschalom, D.P.D. Vincenzo, Complex Dynamics of Mesoscopic Magnets, Physics Today, 48, 43 (1995)
8. R.H. Kodama, A. F.Berkowitz, E.F.M. Niff Jr. S. Foner, Surface Spin Disorder in $NiFe_2O_4$ nanoparticles, Phys. Rev. Lett., 77, 394-397 (1996)
9. M. George, A.M. John, S.S. Nair, P.A. Joy, M.R. Anantharaman, Finite size effects on the structural and magnetic properties of sol-gel synthesized $NiFe_2O_4$ powders, J. Magn. Magn. Mater., 302, 190-195 (2006)
10. C.N. Chinnasamy, A. Narayanasamy, N. Ponpandian, K. Chattopadhyay, H. Guerault, J.M. Greneche, Ferrimagnetic ordering in nanostructured zinc ferrite, Scripta Mater., 44, 1407-1410 (2001)
11. H. Ehrhardt, S.J. Campbell, M. Hofmann, Structural evolution of ball-milled $ZnFe_2O_4$, J. Alloys Comp., 339, 255-260 (2002)
12. T. Kamiyama, K. Haneda, T. Sato, S. Ikeda and H. Asano, Cation distribution in $ZnFe_2O_4$ fine particles studied by neutron powder diffraction, Solid State Commun., 81, 563-566 (1992)
13. T. Sato, K. Haneda, M. Seki, T. Iijima, Morphology and magnetic properties of ultrafine $ZnFe_2O_4$ particles, Appl. Phys. A, 50, 13-16 (1990)
14. M.Hofmann, S.J. Campbell, H. Ehrhardt, R. Feyerherm, The magnetic behaviour of nanostructured zinc ferrite, J. Mater. Science, 39, 5057-5065 (2004)
15. S.A. Oliver, H:H: Hamdeh, J.C. Ho, Localized spin canting in partially inverted $ZnFe_2O_4$ fine powders, Phys. Rev. B, 60, (5), 3400-3405 (1999)
16. B.D. Cullity, Elements of X-Ray Diffraction, Vol.9, Adisson-Wesley Publishing Company, Reading, MA (1956)
17. S.J. Stewart, S.J.A. Figueroa, J.M. Ramallo, S.G. Marchetti, J.F. Bengoa, R.J. Prado F.G. Requejo, Cationic exchange in nanosized $ZnFe_2O_4$ spinel revealed by experimental and simulated near-edge absorption structure, Phys Rev. B, 75, 073408 (2007)

Recibido: 31.07.07
Aceptado: 20.12.07